

Contribution of Electric Tomography, Chemical and Isotopic Tools to the Understanding of the Resilience and Salinization of Wetlands along the Northern Coast of the Cape-Verde Peninsula: The Case of the Retba Lake

Mansour Gueye^{1*}, Abdoul Aziz Gning², Mapathé Ndiaye², Fatou Diop Ngom¹, Raymond Malou¹, El Hadj Sow¹, Raphaël Sarr¹

¹Département de Géologie Faculté des Sciences et Techniques, Université Cheikh Anta Diop, Dakar, Sénégal

²UFR Sciences de l'Ingénierie, Université de Thiès, Thiès, Sénégal

Email: *sauramalick@gmail.com

How to cite this paper: Gueye, M., Gning, A. A., Ndiaye, M., Ngom, F. D., Malou, R., Sow, E. H., & Sarr, R. (2019). Contribution of Electric Tomography, Chemical and Isotopic Tools to the Understanding of the Resilience and Salinization of Wetlands along the Northern Coast of the Cape-Verde Peninsula: The Case of the Retba Lake. *Journal of Geoscience and Environment Protection*, 7, 36-57.

<https://doi.org/10.4236/gep.2019.79004>

Received: July 26, 2019

Accepted: September 16, 2019

Published: September 19, 2019

Copyright © 2019 by author(s) and Scientific Research Publishing Inc.

This work is licensed under the Creative Commons Attribution International License (CC BY 4.0).

<http://creativecommons.org/licenses/by/4.0/>



Open Access

Abstract

On the northern coast of the Cape Verde peninsula, Lake Retba is one of the few depressions that have preserved its water body due to the drought that plagued the Sahel in the 1960s. The aim of this article is to understand the resilience of the lake to the drought. For this purpose, a deep knowledge of interactions between the different components of the hydro-system, namely: lake, dune tablecloth, ponds and ocean is necessary. The use of electrical resistivity tomography (ETR) and chemical and isotopic tools yielded conclusive results. Electrical tomography of resistivity (ETR) shows throughout the coastal dune a superposition between fresh and salt water, with even a predominance of salt water at the level of the old canal. The chemistry of the major ions and isotopes confirms this contact between the saltwater bison of the sea and the lake by showing a superposition of the fresh/brackish waters on the salty waters of the bevel, which, in turn, are found in the very salty waters influenced by the lake. This translates a feeding of the lake by the sea through the bevel. At the canal level, this feeding is done, on the surface, by means of ponds whose water characteristics show that they constitute an outcrop of the bevel. The freshwater body of the coastal dune that floats on salt water in the form of a lens also flows into the lake. The feeding of the lake, by the sea through the bevel and the ponds, and by the water table, is therefore effective and attested by all the methods used in this work. It allowed the resilience of the lake against the drought. This inflow of seawater into the lake is at the origin of its salinization and

therefore of the salt that settles on the bottom. This study shows that the survival of the lake also depends on safeguarding the ponds located in the north of the lake.

Keywords

Tomography, Isotope, Lake, Ponds, Aquifer, Hydro System, Salinization, Resilience

1. Introduction

Lake Retba is located 35 km east of Senegal's capital, Dakar (**Figure 1**). Its watershed covers an area of 160 km² (**Carn et al., 1976**). The lake was established after post-Nouakchottian marine regression, by isolating the initial lagoon by a spire. The waters are over salted and deposit a salty crust at the bottom of the lake (**Garnier, 1978**), which has been exploited by the population since the 1970s. This mining activity produces 110,000 tons of salt annually and generates profit margins ranging from CFAF 1.5 to 3 billion (**Sarr, 1997**). In addition to this mining activity, there are other activities such as tourism, market gardening and fruit arboriculture. As a result, it plays a significant socio-economic role for the country. It is the only lake, on the north coast, that maintains a permanent running water. However, in recent years, the level of the lake has continued to fall to alarming proportions, threatening all socio-economic activities.

Aware of the importance of this ecosystem, the Senegalese government has integrated the "scientific study of Lake Retba" component into the Mining Sector Support Program (PASMI) financed by the European Union. In fact, the protection of Lake Retba requires a thorough knowledge of the interactions between the various components of the hydro system, such as the lake, the groundwater of the Quaternary sands, the sea and the ponds.

These saline systems are very widespread in arid and semi-arid areas. Their existence requires mainly evaporation higher than precipitations (**Hardie et al., 1978; Langbein, 1961**). Their typology is based on geomorphology; it was established by **Yechieli and Wood (2002)**. In fact, geomorphology distinguishes flat-surfaced systems without obvious depression or permanent running water (e.g., Sebkhas in the Arabic Gulf), from shallow water basins with seasonal expanse running water (e.g., Texas playas) and well-developed water basins containing permanent running water (e.g., Dead Sea) with the absence or presence of marine, underground and/or superficial influence. Retba Lake might belong to the latter system. For hydrogeologists, these salt lakes are the result of the same hydrogeological process influenced by fluctuations in shallow groundwater. As such, they may be active or representative of past hydro-geological conditions (**Yechieli & Wood, 2002**).

The first research specifically devoted to Retba Lake dated back to **Elouard et al. (1975)** and **Elouard et al. (1977)**. This author highlighted and dated the

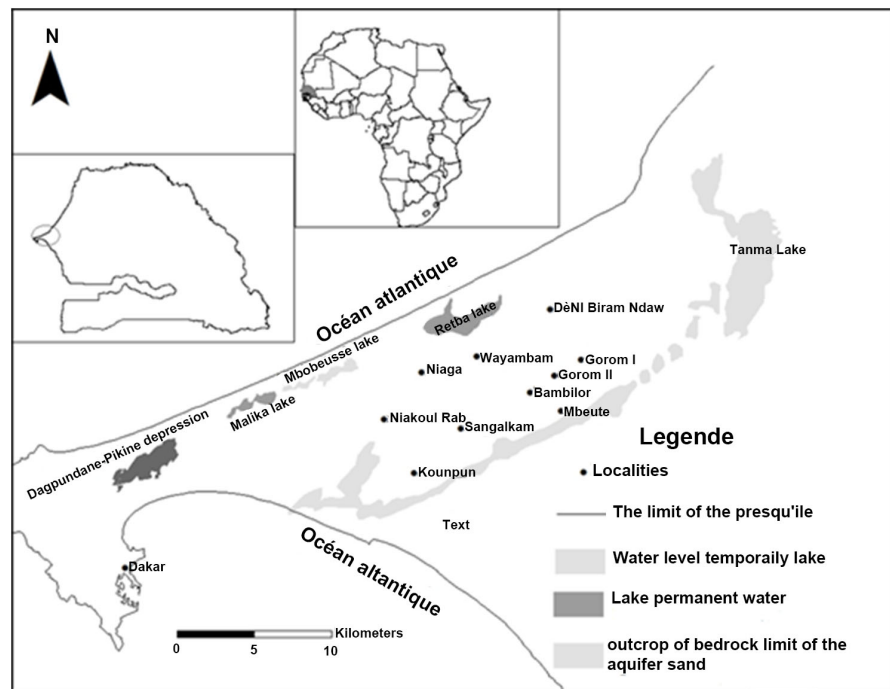


Figure 1. Location of the studied area.

various transgressions and regressions observed in the watershed by dating the dune shells. Recent work by Sarr et al. (2009a) and Sarr et al. (2009b) highlight the paleo-geographic evolution of the lake by integrating biological markers such as molluscs, foraminifera, ostracods and diatoms. According to this author, the lake went through five stages before its current configuration: a slightly open lagoon stage, a small marine gulf stage, a closed lagoon stage in the process of drying out, a slightly open lagoon stage and a closed lagoon stage (lake). The work of Sow et al. (2008) shows an isolation of the lagoon of Retba Lake consecutive from a period of low sea level between 1200 and 250 B.P. They show the seasonal evolution of the ponds' salinity located in the old channel by the use of diatoms, in particular *Paraliasulcata*. Sow et al. (2006) mapped the former supplying routes of the lake by the ocean. This feeding was done in addition to the channel, by another route located North East of the lake. Those of Sarr (1997) point out the diachronic evolution of the water body characterized by a continuous reduction in its surface. The works of Martin (1970), Carn et al. (1976) and Garnier (1978) highlighted the hydrochemistry of lake water in relation to that of the groundwater. These authors consider the lake's hydro-system as fixed, fossilized and non-dynamic. They do not address the ocean-groundwater-lake relationship. They consider the lake's hydro-system as a relic of the salt bevel, with no hydrodynamic relationship with the ocean and evolving in an evaporative tank. This does not explain the lake's resilience to the drought of the 1970s as well as the salinization of its waters. The first studies suggesting that the lake is supplied by the ocean, and therefore having a dynamic system that is being renewed, are those of Gueye et al. (2016). This study corroborates with these first

published results. Its interest lies in the fact that it approaches the hydro-system from a dynamic point of view and updates the knowledge already acquired by the first authors. The purpose of this study is to understand the current functioning of this ecosystem, which led to the salinization of the water and allowed the lake to maintain itself against the drought wave of the 1970s. This helps to identify strategies for managing and safeguarding the resource, that is the salt exploited at lake level by local populations. To achieve this objective, an experimental system composed of four piezometers has been set up on the coastal dune separating the lake and the ocean. A stratified sampling of the groundwater was carried out on these piezometers. The lake and ponds were also sampled. Chemical analyses were performed on the various samples taken from the lake, groundwater and ponds. Three geophysical profiles were carried out to measure the variation of vertical resistivity as a function of depth. Two analyses, on the dune and another on the old channel of the lagoon currently occupied by sandy dunes. These resistivity measurements were performed using the Electric Resistivity Tomography (ETR) method.

2. Presentation of the Studied Area

2.1. Hydrogeological and Hydrological Context

The hydrogeology of the area is dominated by the quaternary sands. These formations, whether marine or continental, behave hydro geologically as a single reservoir directly in contact with the ocean to the west (Vallet, 1972), and its waterproof is variable and depends on the nature of the aquifer formations (Martin, 1970). According to Garnier (1978), the offshore groundwater flows on one hand to the ocean and on the other hand to the lakes.

Permeability is highly variable, as well as transmissivity which is between $5.2 \cdot 10^{-4}$ and $5.6 \cdot 10^{-3}$ m²/s. In Niakoul Rap and Bambilor located in the southern part of the catchment area (Figure 1), it is respectively $2.3 \cdot 10^{-3}$ m²/s and $1.8 \cdot 10^{-3}$ m²/s. The storage coefficient is close to 1%, but can vary due to the presence of some of the more clayey horizons found in the sands. In some areas, the groundwater acquires a semi-captive behavior due to these clayey horizons (Vallet, 1972).

Hydrologically, the lake is fed by rivers that are not sustainable and only operate during the rainy season. It should be noticed that there are two ponds located in the north of the lake below the dune. The water from these ponds flows out and forms a stream that feeds the lake all year round.

2.2. Climate

2.2.1. Temporal Rain Variability

The analysis of rainfall is based on a series of data collected between 1900 and 2013 by ANACIM (National Agency for Civil Aviation and Meteorology). This analysis refers to the normal 1951-1980. In fact, it is the reference of the World Meteorological Organization (WMO) from which climate regimes are analyzed

(Ferry et al., 1998; Ouédraogo, 2001).

In consideration to the normal 1951-1980, the series can be divided into two periods (**Figure 2**) according to the evolution of the rainfall index: a period from 1900 to 1969 and a period from 1970 to 2013:

- The period from 1900 to 1969

The evolution of rainfall indices (**Figure 2**) shows surplus rainfalls that vary between 1% (1900) and 83% (1918, 1951). However, deficit years are noticed, these deficits are between 2% and 49%, and therefore not exceeding 50% of the normal benchmark. This period is therefore generally humid.

- The period from 1970 to 2013

During this period, the number of years in deficit is much higher than the number in surplus ones. Rainfall deficits range from 63% (1970) to 2% (2006) while rainfall surpluses range from 3% (1985) to 33% (2005) and therefore do not exceed 50% compared to the normal 1951-1980. Due to this high rainfall deficit, this period is considered dry.

The five-year moving average in this period shows an alternation of small periods of deficit and surplus, called deficit and surplus cycles. From 1970 onwards, deficit periods became widespread and drought settled.

2.2.2. Evaporation

The yearly average amassings calculated over the period 1970-2002 are 1428 mm/year according Thornthwaite's method and 1469 mm/year using the Turc's method. Cumulating vary between 1458 and 1493 mm per year. These values are similar to those given by authors such as Henry (1972), Vallet (1972) and Lenclud (2005) who estimate that evapotranspiration varies between 1500 mm and 2200 mm per year in the Cape Verde Peninsula.

From this analysis, we can conclude that our area has been marked by drought and high evaporation since the 1970s. These factors combined should lead to the disappearance of surface water bodies. This is not the case for Retba Lake, hence the importance of observing its functioning which allowed its resilience.

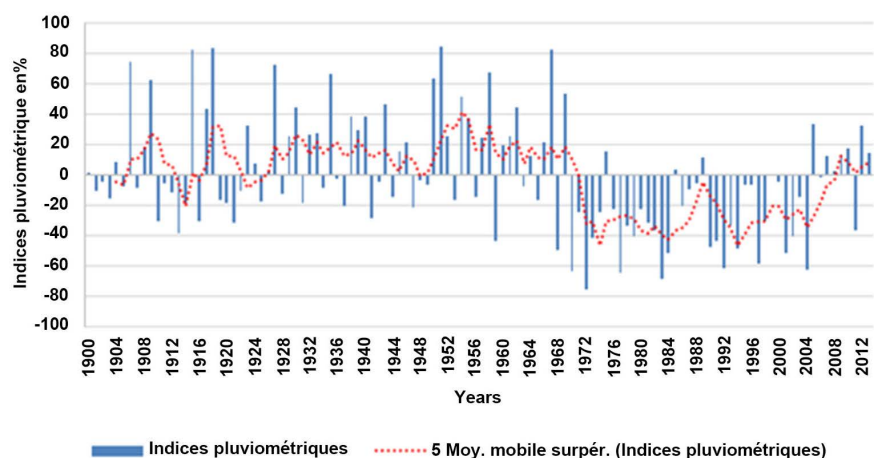


Figure 2. Evolution of rainfall deviations from normal 1951-1980.

3. Materials and Methods

3.1. Electrical Resistivity Tomography (ERT)

3.1.1. Theory and Basic Formulas

For four electrodes, for instance an AB-MN quadrupole of any geometry, the principle of potentials' additivity allows to write (Equation (1)):

$$\Delta V_{MN} = \frac{\rho I_{AB}}{2\pi} * \left[\frac{1}{r_{AM}} - \frac{1}{r_{AN}} - \frac{1}{r_{BM}} + \frac{1}{r_{BN}} \right] \quad (1)$$

In the field, the resistivities' distribution is generally heterogeneous and anisotropic. Thus, an apparent resistivity ρ_a (in ohm-m) is like the resistivity equivalent to a homogeneous and isotropic environment. This apparent resistivity ρ_a (in ohm-m) is given by the following relationship (Equation (2)):

$$\rho_a = K * \frac{\Delta V_{MN}}{I_{AB}} \quad (2)$$

where $K = \frac{2\pi}{\left[\frac{1}{r_{AM}} - \frac{1}{r_{AN}} - \frac{1}{r_{BM}} + \frac{1}{r_{BN}} \right]}$.

K is therefore a factor that only depends on the configuration of the quadrupole geometry (ABMN): It is the geometric factor. Apparent resistivity is the variable measured in the field in direct current electrical prospecting and tomography. It does not directly reflect the actual resistivities or depths of the subsoil materials. As a result, the data measured in the field are processed using inversion software to calculate the true resistivities of the materials: it is inversion or deconvolution. It allows having a section of the basement in true resistivities that will be interpreted.

3.1.2. Application in the Coastal Dune

Using an LS ABEM terrameter, three ETR profiles were performed on the coastal dune between the ocean and the lake. The first two profiles are juxtaposed and have a line length of 630 m of cable from the beach to the approach of the lake (**Figure 3**). The other profile was installed in the old channel of the lake that fed the lagoon (**Figure 3**). The profile is transverse to the channel and measures 210 m from the beach to the depression of the old channel that include pond 2. The device used is the Wenner. The topographic altitude of all electrodes in the three profiles was determined using a differential GPS (Global position system). These data were acquired after the wet season (September 2, 2015) in order to benefit from the moisture in the sands, which facilitates the passage of the current into the deep layers.

3.1.3. Data Processing and Inversion

The RES2DINV software version 3.54.44 was used for data processing and cutting of real resistivity. Once the data has been pre-processed, the modeling parameters are selected before loading the file into the RES2DINV program. For this work, the inversion was performed with an application of the L1-normed



Figure 3. Location of ETR profiles on the coastal dune (Source: Google Earth).

constraint (robust inversion), which implies a more restricted Laplacian distribution of data errors (Al-Chalabi, 1992). The use of a lower standard (L1) is required with data affected by non-random noise.

The quality of the acquisition is checked by visualizing the file where the different levels are represented with a reduced scale (Figure 4). This representation highlights measurements with very low or very high apparent resistivity in relation to neighboring points. Since such a rapid change cannot be due to a geological phenomenon, such data must be eliminated (Maresscot, 2008).

The data acquired are homogeneous since the contact problem did not arise due to the humidity of the dunes. This is illustrated by Figure 4, which shows the acquisition of profile 1 data. After saving the processed file, its modeling inversion is started. The result is subsurface sections representing the vertical and horizontal variation of resistivity. It is these sections that are presented in the result section in the form of profiles.

3.2. Chemical Data Acquisition

3.2.1. Sampling

A line of four piezometers (PA, PB, PC and PD) (Figure 5) was completed on the coastal dune between the lake and the ocean. Sampling was carried out at the end of the wet season, in September 2012. It covered the waters of the dune groundwater as well as surface waters (lake, ponds) and the ocean. During this sampling, a water stratification test was carried out. It consists of sampling at different depths, from the surface to the bottom of the structure, using an Eijkelkamp submersible pump. The structure is first drained and left to rest before all these operations. Three samples are taken at each of the sampling horizons. The physico-chemical parameters (salinity, conductivity, temperature) are also measured with a 315i WTW conductivity meter. The pH is measured with a



Figure 4. Acquisition of profile 1 data, verification of the quality of the acquisition.



Figure 5. Location of PA, PB, PC and PD piezometers on the coastal dune (Source: Google Earth).

Merk pH liquid indicator kit (1.111.07). The samples are pre-filtered in situ with a 0.2 μm filter and then filtered with a 45 μm membrane.

3.2.2. Ion Analysis

In the laboratory, the chemical composition was determined by ion chromatography with a Dionex DX 1100/2100 for cations and major anions (Jackson, 2006). Total inorganic carbon contents are determined by oxidation at high temperature. For anions, analyses were carried out on phosphates (PO_4^-), chlorides (Cl^-), bromides (Br^-), fluorides (F^-), bicarbonates (HCO_3^-), and nitrites (NO_2^-). Cation analysis is carried out on calcium (Ca^{2+}), potassium (K^+), magnesium (Mg^{2+}), ammonium (NH_4^+), sodium (Na^+) and lithium (Li^+).

3.2.3. Isotope Analyses

The stable isotope contents of water ^{18}O and ^2H were measured as follows: 5 ml of sample were distilled at a temperature of 90°C, and then at 105°C for one hour in an Evapoclean, which is a closed evaporation device; this device avoids a high salt concentration for subsequent analysis of the stable isotopes. The oxygen-18 and deuterium contents, were determined using a Picarro L1102i WS-CRDS (Digital Wavelength Ring Cavity Spectroscopy System), as described by Halder and Decrouy (2013). Each sequence was calibrated using three differ-

ent internal standards, which are periodically calibrated to international standards (standards): V-SMOW (Vienna Standard Mean Ocean Water) and SLAP (Standard Light Antarctic Precipitation, characterized by very low levels of oxygen-18 and deuterium) which are IAEA (International Atomic Energy Agency) standards. The isotopic compositions measured are reported in delta units (deviation expressed in ‰) from the isotopic ratio of the sample to that of V-SMOW, standardized so that SLAP has a $\delta^{18}\text{O} = -55.5\text{‰}$ and a $\delta^2\text{H} = -428.0\text{‰}$ (Coplen, 1994; EOS, 1996). The uncertainties on repeated measurements, standards and samples are $\pm 0.1\text{‰}$ for oxygen -18‰ and $\pm 1.4\text{‰}$ for deuterium.

4. Results and Discussions

4.1. Electrical Resistivity Tomography (ERT)

Two transects were carried out: the Dune's transect, consisting of profiles 1 and 2, and the channel's transect, consisting of profile 3. The profiles are south (lake side) to north (ocean side) oriented. Profiles 1 and 2 are successive.

4.1.1. The Dune's Transect

Profile 1: The true resistivity model of this profile (Figure 6), obtained after inversion of the apparent resistivities, with an RMS error of 4.9%, shows five contrasting sets:

1) A superficial unit whose minimum resistivities are around 1000 Ohm-m and maximum resistivities exceeding 6000 Ohm-m. This set corresponds to the dry sands of the dune, which constitute the very resistant dune cover. Its thickness varies between 2 and 3 m.

2) A resistant unit, with resistivities of around 500 Ohm-m. This set is observed just after the very resistant superficial set. This sudden fall in resistivity suggests that this set corresponds to wet sands, i.e. the unsaturated area. This layer is very thin, about 0.5 m thick.

3) A moderately resistant unit, with resistivities between 40 and 200 Ohm-m. According to Archie's law, the resistivities of the imbibition water vary between 8 and 40 Ohm-m. These resistivities translated into conductivities give a range of conductivities that are from 250 to 1250 $\mu\text{S}/\text{cm}$. This set corresponds therefore to the sandy fresh water table of the dune's cordon. According to this profile, its maximum thickness is located at 560 m from the ocean and it is 18 m.

4) A moderately conductive unit, with resistivities between 10 and 40 Ohm-m. According to Archie's law, the resistivities of the imbibition water vary between 2 and 8 Ohm-m. These resistivities, translated into conductivities, give a range of conductivities ranging from 1250 to 5000 $\mu\text{S}/\text{cm}$. This set could therefore correspond to the transition zone between the underlying highly conductive set and set three.

5) A highly conductive set of resistivities between 1 and 10 Ohm-m. According to Archie's law, the resistivities of the imbibition water of this set vary between 0.2 and 2 Ohm-m. The conductivities, obtained from these resistivities, therefore

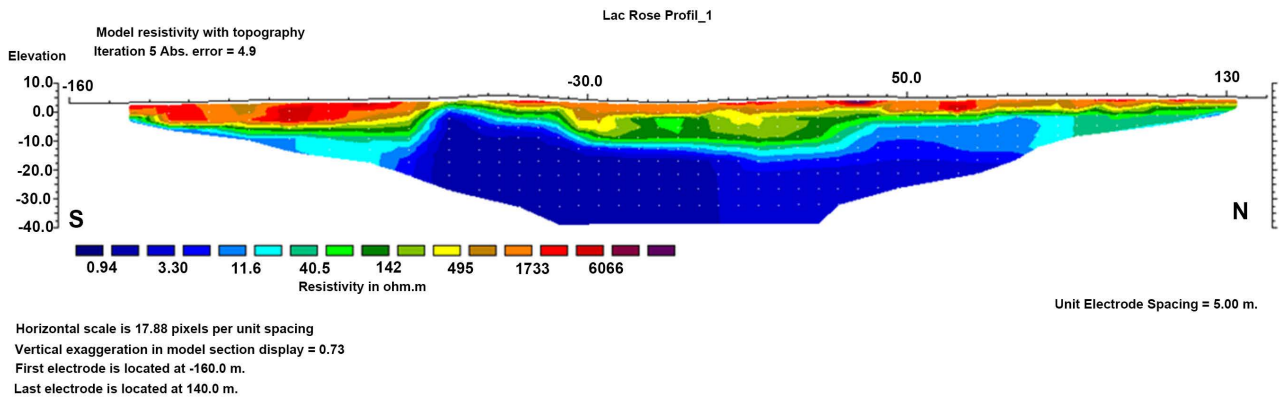


Figure 6. Section of true resistivities, obtained on the coastal dune between the ocean and the lake, inversion carried out with application of the L1-normed stress (robust inversion).

vary between 5000 and 50,000 $\mu\text{S}/\text{cm}$. This set corresponds to the saltwater sands of the coastal dune.

The lateral variation in resistivity observed in each set could be explained by a variation in the proportion of clay in the sands or by the variation in the salinity of the imbibition liquid, in this case, water.

Profile 1 illustrates well the contact between freshwater and salt water and shows that it is a slope that sinks into the dune and then rises towards the ocean. The fresh water's highest thickness is 18 m at a point located at 560 m from the ocean. It also shows that fresh water forms a weak lens over salt water.

Profile 2: This profile was inverted with an RMS error of 13%, probably due to the low signal/noise ratio. Four contrasting sets have been identified (Figure 7):

1) A very resistant unit with resistivities higher than 2000 Ohm-m and which corresponds to the very dry sandy cover;

2) A moderately resistant assembly with resistivities between 35 and 130 Ohm-m. By applying Archie's law, the resistivity of the imbibition water varies between 7 and 26 Ohm-m. This resistivity range gives a conductivity range around 384 to 1428 $\mu\text{S}/\text{cm}$. This set corresponds therefore to the fresh water/brackish sand table of the dune seam, since this profile was closer to the ocean than the first one, which explains why the resistivities of the water are lower, compared to those of the whole profile 1;

3) A highly conductive set of resistivities between 1 and 8 Ohm-m. Based on Archie's Law, the resistivities of the imbibition water obtained vary between 0.2 and 1.6 Ohm-m. This range of resistivities, translated into conductivities, gives conductivities that vary between 6250 and 50,000 $\mu\text{S}/\text{cm}$. This unit corresponds therefore to the salt-water sand table identified on the first profile; the higher conductivities than on the first profile are explained by the proximity of the ocean;

4) A moderately conductive set of resistivities around 20 Ohm-m, which corresponds to the transition zone between the salt-water sand sheet and the fresh water/brackish sand sheet of the dune channel;

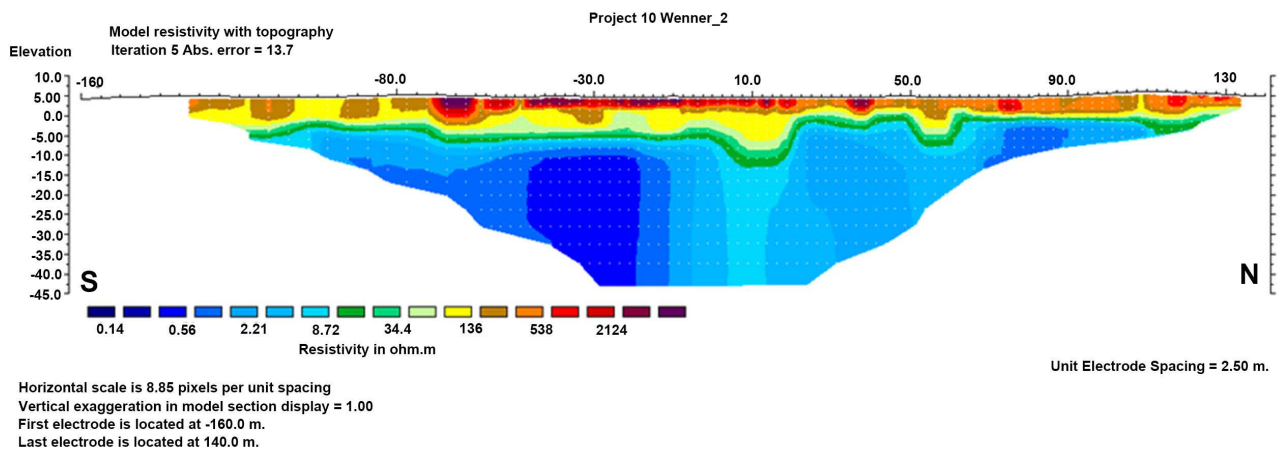


Figure 7. Section of true resistivities, obtained on the coastal dune between the ocean and the lake, inversion carried out with application of the stress L1-standardized (robust inversion).

At the last level, lateral variation of the resistivity is noted. It may also be due to the variation in the proportion of clay in the aquifer sands or to changes in the resistivity of imbibition water or both.

On profile 2 (**Figure 7**), the freshwater-salt water contact occurs from the south to the north towards the ocean. This profile extends the first, so the recovery observed at the first level continues. This shows that the thickness of the freshwater sands aquifer is becoming increasingly weak by moving to the ocean, as shown in **Figure 7**.

4.1.2. The Channel Transect

The channel profile was reversed with a 20% RMS error. However, our knowledge of the field allowed us to interpret it as it was considered fairly consistent with our observations on the ground. Three contrasted sets have been identified (**Figure 8**):

- 1) A very resistant set with resistivities above 1100 Ohm-m; this set corresponds to the sandy, very resistant cover of the dunes.
- 2) A moderately resistant set with resistivities between 50 and 250 Ohm-m. The resistivities of the imbibition water obtained from Archie's law therefore vary between 10 and 50 Ohm-m. These resistivities translated into conductivities give a range of conductivities ranging from 40 to 1000 $\mu\text{S}/\text{cm}$. This set corresponds to the freshwater/brackish water table. Its thickness decreases towards the ocean and is almost cancelled at the end of the profile (north side). Along the profile, small freshwater/brackish lenses are noted.
- 3) A very conductive set with very low resistivities, ranging from 0.024 to 11 Ohm-m. Water resistivities, obtained from Archie's Law, vary between 0.0048 and 5 Ohm-m. These resistivities translated into conductivity give a range of conductivities ranging between 200 and $2.08 \cdot 10^5$ mS/m. This set corresponds to the very salty water sands of the channel. These very high conductivities, suggesting a high salinity, could be explained by the fact that this area corresponds to the old channel and therefore there is an ancient salinity added to the current

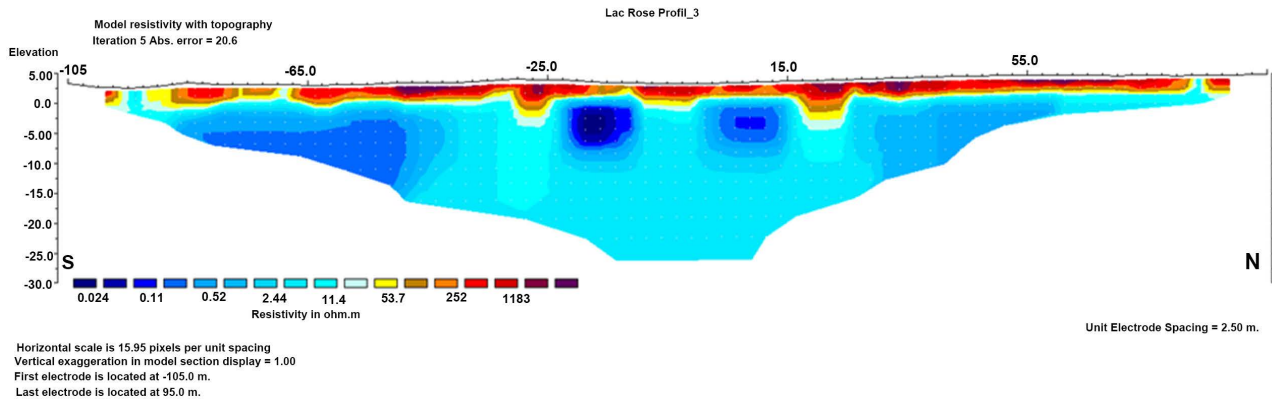


Figure 8. Section of true resistivities, obtained on the coastal dune between the ocean and the lake at the site of the old channel, reversal made the application of the stress L1-standardized.

salinity due to the existence of the bevel. In the southern part it is noted an area of very low resistivity compared to the rest, these very low resistivities may be due to infiltration into the water table, the very salty pond or to clay enrichment, sands, next to the pond2.

On this profile (**Figure 8**), a slight north-south slope, i.e. from the ocean to the pond2, with a gradient of 0.0125 is observed. Pond2 is located at an altitude of -1.47 m, pond 1 to -3 m and the lake at -5.52 m. This shows a gradient from the ocean to the lake and promotes the flow of the bevel to the lake through both ponds. This result is consistent with the work of (Yechieli & Wood, 2002) on coastal saline hydrosystems and their relationship to the ocean. The freshwater/brackish water table does not appear immediately as a lens as seen at the profile level, which is probably due to its low thickness. However, small lenses are observed along the profile.

These results are almost consistent with those of (Comte, 2008), obtained by applying electric tomography to the Pikine-Dagoudane depression site, located west of the lake. Resistivity values also fall within the scale given by Debuissou (1965) and Moussu and Debuissou (1966). These geo-electric profiles show that between the lake and the ocean, there is a salty or even very salty water table that connects the lake to the ocean. This water table is overcome by the fresh/brackish water table of the dune cord. The maximum thickness of this fresh/brackish water table does not exceed 20 m. This maximum thickness is observed at a position 560 m from the ocean. From this position, the thickness of the table decreases by heading towards the lake and the ocean. The fresh water table floats on that of salt water table as a lens. However, it is not as powerful as it is to create a hydraulic barrier that prevents the lake from eating by the ocean, as reported (Garnier, 1978). Indeed, the lens is not capable of repelling the fresh water-salt water interface according to the proportions predicted by the law of Ghyben-Herzberg. Piezometric levels, measured on piezometers, show that the water table is below ocean level.

The ETR profile performed on the old channel shows that the fresh/brackish waters of the groundwater table at channel level is based on the salt waters of the

bevel. There is a clear predominance of salt water from the sea over fresh water from the dune groundwater at the channel level. Geophysics therefore shows the existence of a salt water table extending from the sea to the pond². Sea water, in the form of a salt bevel, flows under the dune and starves into the depression of the old channel that forms the pond². This pond in turn feeds the lake. This shows that this channel still operates underground.

4.2. Vertical Evolution of Dune Groundwater Chemistry

During September 2012, a stratified sampling, at different depths, of the waters of the four coastal dune piezometers was performed in order to better understand the vertical evolution of their chemistry and compare it with that of the ocean on the one hand and with that of the ponds and lake on the other hand.

Salinity increases with depth at the PA and PD piezometers. In the PA, it goes from 15 g/l (at a depth of 2.75 m), to 19 g/l (at 4.5 m). At PD, it is 3.5 g/l (at 4.5 m depth), and 31 g/l (at 7.5 m depth). Chlorides are also high in the waters of these two structures and increase with depth. In the PA, they are between 231 and 298 meq/l and between 44 and 557 meq/l in the PD. The salinity measured at the water level of the PB and PC piezometer samples is zero.

The piezometers, PA and PD capture a salt water table and the PB and PC piezometers, about 5 m deep, capture the fresh water sand table. These piezometers located in the middle of the dune capture the freshwater lens trapped on either side by the salt water collected by the PA and PB piezometers.

4.3. Principal Component Analysis (PCA)

Choice of the main components

We choose to study only the two main components. The choice of these main components is justified by the histogram of variances according to the different components (**Figure 9**) on which the scree curve is drawn (red curve). This curve shows that the axes associated with the eigenvalues before the break represent the largest variance. These are axis 1 (Dim1) and axis 2 (Dim 2).

These two main components (axis1 and axis2) (**Figure 10, Figure 11**) account for 79.33% of the total variability, of which axis1 explains nearly 58.14% of the variations and axis2 25.24%. This reflects the quality of the data since only 20.67% of the information is lost. The factorial design will therefore consist of these two axes. The analysis will be carried out according to these two axes.

Study of the cloud of variables

The representation of the variables on the correlation circle (**Figure 10**) shows that there are two groups of variables:

The group of variables whose vector ends representing them is all very close to the circle of correlations or is on its boundary. These variables are significant and well represented. The qualities of the representations of these variables are satisfactory. These variables are: distance, altitude, conductivity (cond), bicarbonate (HCO_3^-), ammonium (NH_4^+), bromide (Br^-), deuterium (^2H), oxygen-18

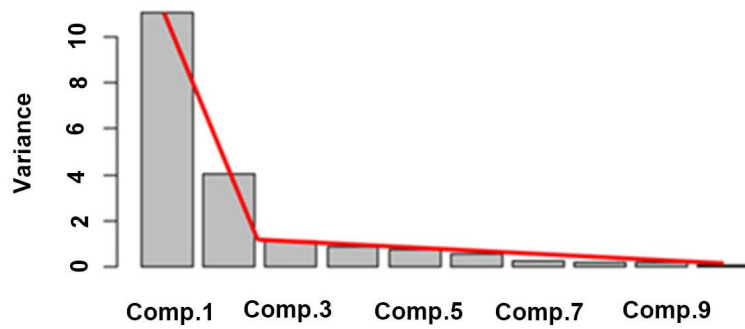


Figure 9. Histogram of variances according to the different components.

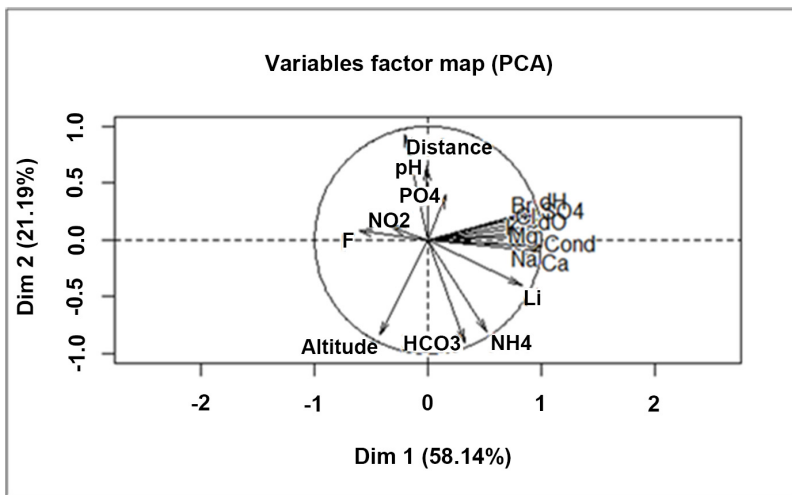


Figure 10. Circle of correlations of variables.

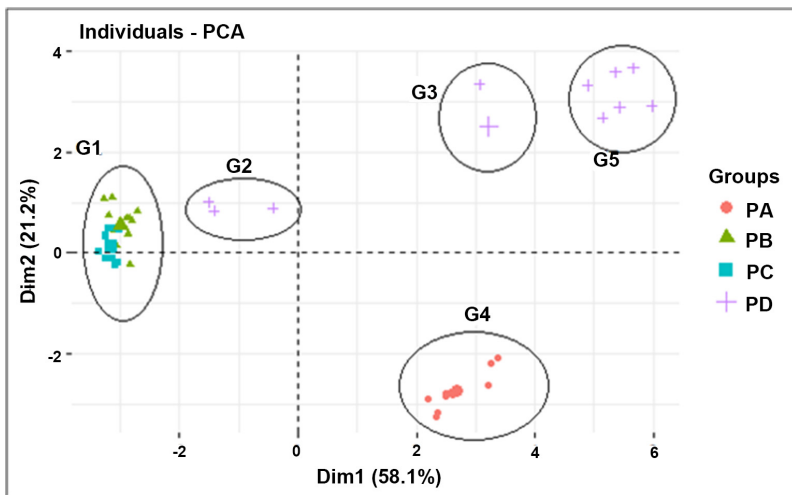


Figure 11. Projection of water samples from the PA, PB, PC and PD piezometers on the factorial plan (Dim 1, Dim 2).

(¹⁸O), magnesium (Mg²⁺), sodium (Na⁺), calcium (Ca²⁺), chlorine (Cl⁻) and sulphate (SO₄²⁻).

The group of variables whose vector ends representing them is close to the

origin (i.e. 0). These variables are not significant and are therefore poorly represented. These are nitrite (NO_2^-), phosphate oxide (PO_4^{2-}), pH and fluorine (F^-). These variables will not be included in the analysis since they do not contribute to the variance of the chemical composition of the water.

The variables: conductivity (cond), bicarbonate (HCO_3^-), ammonium (NH_4^+), bromine (Br^-), deuterium (^2H), oxygen-18 (^{18}O), magnesium (Mg^{2+}), sodium (Na^+), calcium (Ca^{2+}), chlorine (Cl^-) and sulfate (SO_4^{2-}) are strongly correlated with axis 1 (Dim 1). These variables therefore contribute to the formation of this axis. They are strongly correlated with conductivity. On the other hand, the variables altitude and distance (from the sea) are not correlated with this axis. This axis (Dim 1) therefore contrasts the variables that contribute to salinity with those that do not. It thus defines a salinity gradient.

Study of the cloud of individuals

The projection of the individuals (samples) on the factorial plane consisting of axis 1 and axis 2 gives **Figure 11**. It shows that the individuals (sample waters) can be separated into five groups: G1 (sample waters from PB and PC piezometers), G2 (surface waters from the first three samples from the PD piezometer), G3 (intermediate waters from the two samples from the PD piezometer), G4 (sample waters from the PA piezometer) and G5 (deep waters from the PD piezometer). Individuals in groups G1 and G2 have negative coordinates on axis 1 (Dim 1) and those in groups G3, G4 and G5 have positive coordinates on the same axis. Samples of groups G3, G4 and G5 therefore have higher values for the following variables: conductivity (cond), bicarbonate (HCO_3^-), ammonium (NH_4^+), bromine (Br^-), deuterium (^2H), oxygen-18 (^{18}O), magnesium (Mg^{2+}), sodium (Na^+), calcium (Ca^{2+}), chlorine (Cl^-) and sulfate (SO_4^{2-}) than those of groups G1 and G2. Axis 1 therefore contrasts individuals in groups G1 and G2 who have low to zero salinity with individuals in groups G3, G4 and G5 who have high salinity. This axis therefore represents salinity. It thus defines a salinity gradient, ranging from fresh/brackish water, consisting of the waters of the PC and PB piezometers and the waters of the first three surface samples of the PD piezometer, to salt water, consisting of the waters of the deep and intermediate samples of the PD piezometer and the PA piezometer. The factorial design shows that the surface water of the PD piezometer is closer to the water of the PB and PC piezometers. These waters are representative of the freshwater/brackish sand table of the barrier boom. The waters of the intermediate samples of the PD piezometer (G3) are closer to the waters of the PA piezometer samples (these samples have coordinates between 2 and 4 on axis 1) which are under marine influence due to their proximity to the ocean. These intermediate waters are therefore influenced by the level of the sea. The deep sample waters of the PD piezometer stand out completely from the other groups with coordinates between 5 and 6 on axis 1 (Dim 1). These waters therefore show a high salinity higher than that of the waters of the PA piezometer, which is closer to the sea. This salinity is therefore justified by a lacustrine influence. The water from the lake seeps into the dune, increasing the salinity of these waters.

From this analysis, it appears that at the level of the coastal dune, there are three types of water: the fresh/brackish water table represented by groups G1 and G2, the salt water table of the sea level represented by groups G3 and G4 and the very salt water table represented by group G5. Groups G2, G3, G5 are waters of the piezometer PD. Therefore, at the level of this piezometer we note a stratification of these three types of water. This piezometer contains water from the water table of the coastal dune (fresh/brackish water) which is found on the waters of the sea level, which rests on the very salty water probably coming from the lake level. This shows a continuity of the sea level at the level of this piezometer and a superposition of ocean waters on the lake waters.

4.4. Isotopic Study of the Waters of the Groundwater of the Coastal Dune

4.4.1. Relationship $^{18}\text{O}/^2\text{H}$

The $^{18}\text{O}/^2\text{H}$ relationship of the dune sand water table, captured by the PA, PB, PC and PD piezometers, is aligned with a right of equation $y = 6.5x - 0.7$ with a correlation coefficient of 0.99 (Figure 12). The slope of the regression right is equal to 6.5; it is 8 for the world meteoric waters and 7 for the local one. This shows that these waters have slightly evaporated. The sample distribution includes the five groups determined from the CPA:

G1 and G2 groups: the waters of the samples have oxygen-18 levels, which vary between -5.6 and -4.3 . Deuterium content varies between -33.9 and -30.6 . The waters of the samples of these groups plow on the local meteorological right, traced through the isotopes of local rainwater by Diouf (2012). They are therefore an isotopic signal close to that of rainwater. They are representative of the freshwater table of the coastal dune.

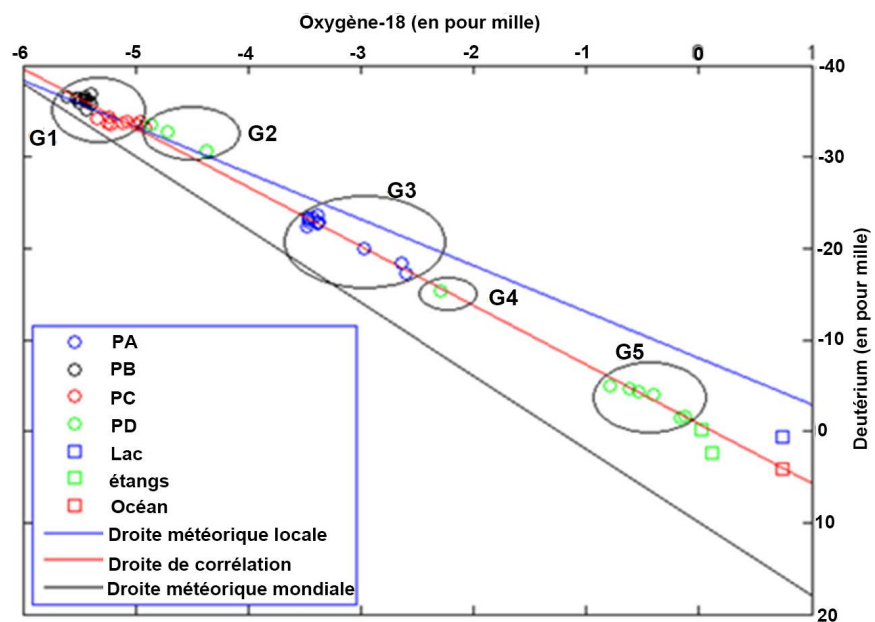


Figure 12. Distribution of deuterium base on oxygen from piezometers PA, PB, PC and PD.

Groups G3 and G4 consisting of PA piezometer samples with 18 oxygen levels varying between -3.4‰ to -2.6‰ and those in deuterium vary between -17.3‰ to -23.3‰ and the intermediate sample of the PD piezometer oxygen 18 and -2.29‰ , deuterium content is -15.3‰ . Their oxygen-18 content is close to that of seawater, which is 0.73‰ . The fraction of sea water in water under marine influence may be calculated by the following formula (Equation (3)) (Appelo & Postma, 2005):

$$f_{\text{seawater}} = \frac{M - m}{S - m} \times 100 \quad (3)$$

With f_{seawater} = fraction of seawater in percentage, M is the mmol/l concentration of the sample chloride, m is the concentration of chloride ions in mmol/l freshwater, S is the concentration of chloride ions in mmol/l of seawater.

For the groups G3 and G4 groups the fraction of seawater varies between 31 and 51%. This shows that the groundwater at the level of the PA piezometer is under marine influence as well as the water at the intermediate level of the PD piezometer.

The G5 group consists of the waters of the deep samples of the PD piezometer. Their oxygen-18 content varies between -1‰ and 0‰ and those of deuterium between -10‰ and -1.5‰ while the oxygen-18 levels content of PB and PC piezometers vary between -5.6‰ and -4.9‰ and deuterium of these piezometers varies between -36.9‰ and -33.2‰ . The lake has 18 oxygen levels ranging from 0.7‰ and 1‰ and deuterium levels ranging between 0.6‰ and 1‰ . The deuterium content of seawater is 4.2‰ and that of oxygen-18 is 0.7‰ . This shows, on the one hand, that the waters of the lake have an isotopic signature near those of seawater and that the deep waters of the PD piezometer are close to those of the lake. These waters are influenced by lake waters that infiltrate the dune.

This isotopic study confirms the distribution of the groups displayed by the CPA and the relationship between G1 and G2 groups and between G3 and G4 groups on the other. It also confirms that the G5 group's waters do not belong to the same type as the other representative groups of the groundwater (fresh and salty); these waters are closer to the lake. This confirms the stratification of the waters at the level of the PD piezometer where the water of the fresh/brackish dune groundwater (G1 and G2) which is based on water from the sea level (G2 and G3) which in turn is based on very salty water (mixing water of the sea and water of the lake) (G5).

4.4.2. Deuterium/Chloride Relationship

The "heavy isotopes/chlorides" relationship and the discretization of the samples based on their depth of sampling also the identification of sample groups identified by the PCA:

It is a question of:

G1 and G2 groups: G1 group has low deuterium levels (ranging from 36.9‰ to 33.2‰), with chloride concentrations varying between 1 and 3 meq/l. The G2

group exhibited low deuterium levels (ranging from -33 to -30‰) and chloride concentrations varying from 40 to 55 meq/l. Their deuterium levels are therefore close to that of the G1 group but they have a high salinity.

These waters represent the fresh water table of the coastal dune. The waters of G2 group (surface waters of the PD piezometer) are part of this aquifer but they have been influenced by deep salted waters resulting in relatively large chloride concentrations.

G3 and G4 groups: They have deuterium levels ranging between -25.6 and -15‰ . Their chloride concentrations vary between 200 and 300 meq/l. They are more enriched in deuterium than the waters of the PB and PC piezometers. **Figure 15** confirms the proximity, already seen at the CPA level, between these two groups (G3 and G4) and between these two groups and the seawater sample on the other hand. This shows that these waters are under marine influences and their chloride concentrations corroborate this.

In addition, G5 consisting of the waters of the deep samples of the PD piezometer. They show deuterium that varies between -5‰ and -1.5‰ and chloride levels ranging from 300 to 500 meq/l. Their deuterium isotopic signature approximates those of lake water and their chloride concentrations are closer to that of seawater (**Figure 13**). This confirms the results already reported on the origin of the deep waters of the PD piezometer. These waters have marine origin, but have a lake influenced from the infiltration of lake water into the dune.

According to **Figure 13**, the ponds have an isotopic signature and chloride concentrations close to the seawater sample. This confirms the geophysical results already mentioned: These ponds are an outcrop of the sea's biswater. In addition, the lake's feeding by the sea, at the channel level, passes through these surface ponds, and by the deep biswater.

4.4.3. Relationship between the Br^-/Cl^- Ratio and Chlorides (Cl^-)

The evolution of bromides (Br^-) based on chlorides (Cl^-) (**Figure 14**) showed a strong correlation between Br^- and ions (Cl^-), with a correlation coefficient equal to 0.959. This means that both ions have a common origin or come from the same process.

The Br^-/Cl^- ratio (**Figure 15**) highlights the influence of seawater on the coastal groundwater. This ratio, bromide-chloride, is constant and equal to 3.47×10^{-3} for seawater (Marjoua et al., 1997). When the values of the Br^-/Cl^- ratio of fresh water are close to or greater than 3.47×10^{-3} this translates into a seawater flow into the groundwater. This report is therefore used to identify the saline origin of water (Faye et al., 2005; Marjoua et al., 1997; Richter & Kreitler, 1993; Viviana et al., 2010). The surface waters of the PD piezometer (G2) and the waters of the piezometer PC and PB (G1) piezometers have low Br^-/Cl^- ratios and chloride concentrations (**Figure 15**). For the surface waters of the PD piezometer, the ratio varies between 0.0001 and 0.00038 and their chloride concentration varies between 45 and 50 meq/l and for the PB and PC piezometers, the Br^-/Cl^- ratio varies between 0.00075 and 0.001 whereas their chloride concentration

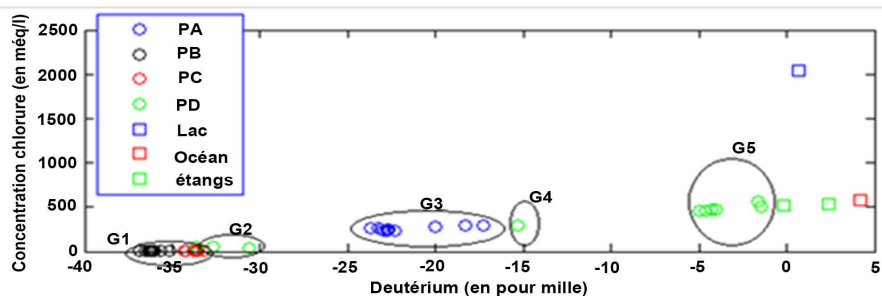


Figure 13. Deuterium vs oxygen ratio of water from wells' samples of PA, PB, PC and PD.

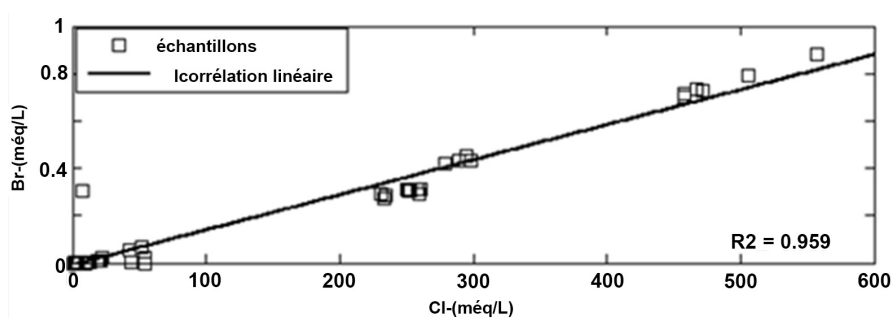


Figure 14. Br⁻/Cl⁻ relationship and chlorides (Cl⁻).

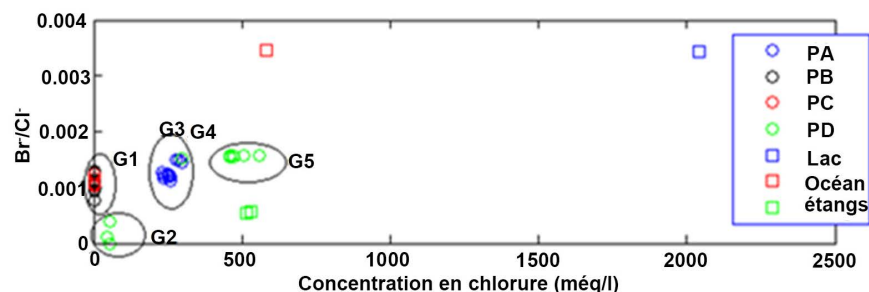


Figure 15. Br⁻ relationship and chlorides (Cl⁻).

varies between 1 and 3 meq/l. By comparing these values with the seawater ratio, it can be said that these piezometers are not or slightly influenced by seawater. The lower chloride values observed at the surface water level of the PD piezometer were explained by its proximity to the lake.

The waters of the PA piezometer (G3) and the waters of the intermediate sample of the PD piezometer have a Br⁻/Cl⁻ ratio ranging from 0.2723 to 0.4552 and chloride concentrations varying between 230 and 300 meq/l. These ratios Br⁻/Cl⁻ higher than that of seawater indicates that the waters of this piezometer are influenced by sea water through its salty biswater.

The deep waters of the PD piezometer have a Br⁻/Cl⁻ ratio that varies between 0.00153 and 0.00157. Their chloride concentration varies between 300 and 500 meq/L. Their Br⁻/Cl⁻ ratios are lower than that of seawater but their chloride concentrations are close to the latter (550 meq/l). This shows that the deep waters of the PD piezometer also have a marine influence by the arrival of the bis-

water at the level of this piezometer. Their isotopic signature also advocates for lake influence.

The water of the lake has a Br^-/Cl^- ratio equal to 0.00344, thus substantially equal to that of seawater. Its chloride content is 2000 meq/l while that of seawater is 550 meq/l. This clearly shows that lake waters are marine waters that have undergone evaporative concentration. These isotopic tools show that this diet passes through the dune via the salt bevel of the sea and from the old channel through the ponds.

5. Conclusion

From these developments, it can be concluded that isotopes, water chemistry, and geophysics have elucidated the operation of the lake's hydro-system. The ocean and the water table of the coastal dune influence the lake. During the dry season, it receives continental inputs. The superposition of "fresh water/salt water table" is also attested by geo-electric models. The same is applied to water chemistry, such as the Br^-/Cl^- ratio, which confirms that the lake's waters are indeed of marine origin. The old channel is also a witness to this lake feeding by the ocean. There is a strong resurgence of salted bevel of the sea in the ponds that mark it. The lake is thus an evaporative pond, the permanent source of which is the ocean and the freshwater lens of the coastal dune. There is such a concentration of water there, by evaporation, that the salinity of its waters reaches 9 times that of seawater. During the rainy season, there is also runoff, through the hydrographic network, which provides a slight softening of the water. In the dry season, the concentration is again triggered. This operation explains the salinization of these waters as well as its resilience to the drought of the 1970s because it has a permanent source of food that is the sea. Protection of the ponds must therefore be taken to prevent the lake from drying out.

Conflicts of Interest

The authors declare no conflicts of interest regarding the publication of this paper.

References

- Al-Chalabi, M. (1992). When "Least-Squares" Squares Least. *Geophysical Prospecting*, 40, 359-378. <https://doi.org/10.1111/j.1365-2478.1992.tb00380.x>
- Appelo, C. A. J., & Postma, D. (2005). *Geochemistry, Groundwater and Pollution*. Rotterdam: A.A. Balkema. <https://doi.org/10.1201/9781439833544>
- Carn, J., Garnier, J. M., & Maglione, G. F. (1976). *Données préliminaires sur les possibilités d'installation d'une saline à l'emplacement du lac Retba, Cap-Vert, Sénégal*. Dakar: Rapport ORSTOM.
- Comte, J. C. (2008). *Apport de la Tomographie Electrique à la Modélisation des Ecoulements Densitaires dans les Aquifères Côtiers: Application à trois contextes Climatique Contrastés (Canada, Nouvelle-Calédonie, Sénégal)*. Avignon: Université d'Avignon et des Pays de Vaucluse.

- Coplen, T. B. (1994). Reporting of Stable Hydrogen, Carbon, and Oxygen Isotopic Abundances. *Pure and Applied Chemistry*, 66, 273-276. <https://doi.org/10.1351/pac199466020273>
- Debuisson, J. (1965). *Analyse des facteurs régissant les contacts eaux-douces-eaux salées dans les sables de la presqu'île du Cap-Vert*. Dakar: Rapp. BRGM 65-A10.
- Diouf, A. (2012). Combined Uses of Water-Table Fluctuation (WTF), Chloride Mass Balance (CMB) and Environmental Isotopes Methods to Investigate Groundwater Recharge in the Thiaroye Sandy Aquifer (Dakar, Senegal). *African Journal of Environmental Science and Technology*, 6, 425-437. <https://doi.org/10.5897/AJEST12.100>
- Elouard, P., Evin, J., & Hébrard, L. (1975). Observations et résultats de mesures au radiocarbonate sur les cordons littoraux coquilliers du lac Retba-Sénégal. *Bulletin de Liaison de l'ASEQUA*, 46, 15-19.
- Elouard, P., Faure, H., & Hébrard, L. (1977). Variations du niveau de la mer au cours des 15 000 dernières années autour de la presqu'île du Cap-Vert, Dakar-Sénégal. *Bulletin de Liaison de l'ASEQUA*, 50, 29-49.
- EOS (1996). *Ratios for Light-Element Isotopes Standardized for Better Interlaboratory Comparison: Transaction*. Washington DC: American Geophysical Union. <https://doi.org/10.1029/96EO00182>
- Faye, S., Maloszewski, P., Stichler, W., Trimborn, P., Cissé Faye, S., & Gaye, C. B. (2005). Groundwater Salinization in the Saloum (Senegal) Delta Aquifer Minor Elements and Isotopic Indicators. *Science of the Total Environment*, 343, 243-259. <https://doi.org/10.1016/j.scitotenv.2004.10.001>
- Ferry, L., L'hote, Y., & Wesselink, A. (1998). Les précipitations dans le sud-ouest de Madagascar. *IAHS Publication*, 252, 89-96.
- Garnier, J., M. (1978). Evolution géochimique d'un milieu confiné: le lac Retba (Cap-Vert) Sénégal. *Revue de Géographie Physique et de Géologie Dynamique*, XX, 13-58.
- Gueye, M., Gning A., A., Ngom Diop, F., & Malou, R. (2016). Hydrodynamic and Hydro-Geochemical Processes in the Catchment Area of Lake Retba and Their Implications in Relationship between Groundwater, Lake and Ocean. *American Journal of Water Resources*, 4, 91-101. <http://pubs.sciepub.com/ajwr/4/4/3>
- Halder, J., & Decrouy, L. (2013). Mixing of Rhône River Water in Lake Geneva (Switzerland-France) Inferred from Stable Hydrogen and Oxygen Isotope Profiles. *Journal of Hydrology*, 477, 152-164. <https://doi.org/10.1016/j.jhydrol.2012.11.026>
- Hardie, L. A., Smoot, J. P., & Eugster, H. P. (1978). Saline Lakes and Their Deposits: A Sedimentological Approach. In A. Matter, & M. E. Tucker, (Eds.), *Modern and Ancient Lake Sediments* (pp. 7-41). International Association of Sedimentologists. <https://doi.org/10.1002/9781444303698.ch2>
- Henry, J. L. (1972). *Etude sur modèle Mathématique du système aquifère de la Presqu'île du Cap-Vert*. Dakar: Rapp. Geohydraulique/O.M.S.
- Jackson, P. E. (2006). *Ion Chromatography in Environmental Analysis. Encyclopedia of Analytical Chemistry*. New York: John Wiley & Sons, Ltd.
- Langbein, W. S. (1961). *Salinity and Hydrology of Closed Lakes*. Geological Survey Professional No. Paper 412. <https://doi.org/10.3133/pp412>
- Lenclud, F. (2005). *Mobilisation de ressources en eau alternatives pour l'irrigation dans la région de Dakar: Etude d'avant-projet détaillé*. Dakar: Cabinet Merlin ingénieurs Conseils.
- Marescot, L. (2008). *Imagerie électrique pour géologue-acquisition, traitement, interprétation*. ETH-Swiss Federal Institute of Technology Zurich.

- Marjoua, A., Olive, P., & Jusserand, C. (1997). Apport des outils chimiques et isotopiques à l'identification des origines de la salinisation des eaux: Cas de la nappe de Chaouia côtière (Maroc). *Revue des sciences de l'eau*, 4, 489-505.
<https://doi.org/10.7202/705290ar>
- Martin, A. (1970). *Les nappes de la presqu'île du Cap-Vert (République du Sénégal): Leur utilisation pour l'alimentation en eau de Dakar, Notice et cartes hydrogéologiques 1/50 000*. France: BRGM.
- Moussu, H., & Debuissou, J. (1966). Etude expérimentale d'un équilibre eaux douces-eaux salées, sur le rivage maritime de Malika, près de Dakar (Sénégal). *Bulletin du BRGM*, 1, 38-65.
- Ouédraogo, M. (2001). *Contribution à l'étude de l'impact de la variabilité climatique sur les ressources en eau en Afrique de l'ouest, analyse des conséquences d'une sécheresse persistante: Normes hydrologiques et modélisation régionale*. Montpellier: Université Montpellier II.
- Richter, B. C., & Kreitler, C. W. (1993). *Geochemical techniques for identifying sources of groundwater salinization*, United States of America, Library of Congress Cataloging-in-publication Data.
- Sarr, F. O. (1997). *Apports de la télédétection et des systèmes d'information géographique (S.I.G) au suivi des zones côtières: Exemple du Lac Retba*. Mémoire d'Ingénieur Géologue, Dakar: Université Cheikh Anta Diop.
- Sarr, R., Debenay, J. P., & Sow, E. (2009a). Sea Level Changes Recorded by Foraminiferal Assemblages in the Upper Holocene of the Retba Lake (Senegal). *Revue de Micropaléontologie*, 52, 31-41. <https://doi.org/10.1016/j.revmic.2007.01.008>
- Sarr, R., Sow, E., & Bodergat, A. M. (2009b). Holocene Marine Incursions in Lac Retba (Cap Vert, Senegal) Evidenced by Ostracod Faunas. *Geobios*, 42, 381-395.
<https://doi.org/10.1016/j.geobios.2008.09.005>
- Sow, E., Compère, P., & Sarr, R. (2006). Diatomées fossiles du lac Retba (Sénégal, Afrique de l'Ouest). Aperçu paléo-écologique. *Algological Studies*, 120, 65-82.
<https://doi.org/10.1127/1864-1318/2006/0120-0063>
- Sow, E., Fofana, C. A. K., Aw, C., & Sarr, R. (2008). Mise en évidence d'une période d'isolement du lac Retba (Sénégal) entre 1200 et 250 B.P. par l'abondance de *Paralia sulcata* (EHRENBERG) Cleve. *Journal des sciences*, 8, 52-58.
- Vallet, P. (1972). *Approvisionnement en eau et assainissement de Dakar et ses environs: Etude des eaux souterraines, Tome II: Etude hydrogéologique de la nappe des sables Quaternaires*. Dakar: Rapport OMS projet Sénégal 3201.
- Viviana, R., Cissé Faye, S., Faye, A., Faye, S., Gaye, C. B., Sacchi, E., & Zuppi, G. M. (2010) Water Quality Decline in Coastal Aquifers under Anthropic Pressure: The Case of a Suburban Area of Dakar (Senegal). *Environmental Monitoring and Assessment*, 172, 605-622.
- Yechieli, Y., & Wood, W. W. (2002). Hydrogeologic Processes in Saline Systems: Playas, Sabkhas, and Saline Lakes. *Earth-Science Reviews*, 58, 343-365.
[https://doi.org/10.1016/S0012-8252\(02\)00067-3](https://doi.org/10.1016/S0012-8252(02)00067-3)